cosmetics

MDPI

Article

Sinomenine from *Sinomenium acutum* Rhizome: A Promising Bioactive Ingredient Associated with Hair-Growth Promotion

Chae Eun Kim [1], Kyong Kim [1], Chae-Heon Lee [1], Eun-Young Park [2], Chul Young Kim [3] and Yoon Sin Oh [1,*]

[1] Department of Food and Nutrition, Eulji University, Seongnam 13135, Republic of Korea
[2] College of Pharmacy and Natural Medicine Research Institute, Mokpo National University, Muan 58554, Republic of Korea
[3] College of Pharmacy and Institute of Pharmaceutical Science and Technology, Hanyang University, Ansan 15588, Republic of Korea
* Correspondence: ysoh@eulji.ac.kr; Tel.: +82-31-740-7287

Abstract

Androgenetic alopecia (AGA) is characterized by disruption of the hair-growth cycle and alterations in growth-related and inflammatory signaling. *Sinomenium acutum* and its major compound, sinomenine (SIN), have been reported to possess antioxidant and anti-inflammatory activities; however, their effects on hair growth regulation remain unclear. Therefore, the aim of this study was to investigate the effects of *S. acutum* rhizome extract (SAE) and SIN on hair cycle transition and explore the associated molecular changes. In vivo and in vitro models were used to determine the effects of SAE and SIN and their correlation with hair-growth-promoting and inhibitory factors, as well as the associated Wnt/β-catenin signaling pathway and inflammatory responses. Sinomenine significantly upregulated the expression of vascular endothelial growth factor, basic fibroblast growth factor, and β-catenin but suppressed that of transforming growth factor-β1, dickkopf-1, and proinflammatory cytokines, which was associated with anagen phase induction. It also showed concentration-dependent effects in vitro at nanomolar concentrations, suggesting that it contributes to the activity of SAE. Histopathological analyses showed an increased number of anagen follicles and improved hair shaft elongation in the treated groups, consistent with enhanced anagen entry. In addition, sinomenine attenuated dihydrotestosterone (DHT)-induced changes in human dermal papilla cells (HDPCs), which were associated with growth factor and inflammatory markers. These findings suggest that SIN is a promising bioactive compound for hair care applications, although further validation is required.

Keywords: androgenetic alopecia; *Sinomenium acutum* rhizome; sinomenine; hair growth factors; Wnt/β-catenin signaling

Check for updates

Academic Editor: Enzo Berardesca

Received: 12 August 2026
Revised: 19 October 2026
Accepted: 19 October 2026
Published: 26 October 2026

Copyright: © 2026 by the authors. Licensee MDPI, Basel, Switzerland. This article is an open access article distributed under the terms and conditions of the Creative Commons Attribution (CC BY) license.

1. Introduction

Hair serves multiple physiological functions in the skin, such as protecting hair follicles and providing thermal insulation [1], and also plays a major role in determining an individual's first impression. Consequently, hair loss exerts detrimental effects on self-confidence and social well-being, often causing depression, emotional distress, anxiety, and social maladjustment [2]. However, hair transplantation mitigates these negative psychological and social consequences, resulting in improvements in quality of life and psychosocial outcomes [3].

The normal hair-growth cycle consists of three distinct phases, viz., anagen, the active growth period; catagen, a short transitional period; and telogen, a resting stage lasting approximately 3 months, during which the hair follicle migrates toward the epidermis and the hair shaft is shed. Subsequently, a new anagen phase begins, initiating the renewal of the hair-growth cycle [4]. In alopecia, the catagen and telogen phases are prolonged, whereas the anagen phase is shortened; consequently, hair shafts become progressively miniaturized due to insufficient growth during the anagen phase [5].

Among the various types of alopecia, androgenetic alopecia (AGA) is the most common cause of hair loss in men. AGA is primarily induced by excessive dihydrotestosterone (DHT), which is synthesized by 5α-reductase and contributes to follicular miniaturization by shortening the anagen phase [6]. Excessive DHT dysregulates multiple molecular pathways involved in hair follicle homeostasis, including increased expression of inhibitory factors such as transforming growth factor (TGF)-β1 and decreased expression of growth-promoting factors such as vascular endothelial growth factor (VEGF) [7]. Furthermore, hair follicle cycling is regulated by crucial signaling networks, including Wnt/β-catenin signaling, as well as inflammatory cytokine-mediated microenvironmental changes, which have been implicated in follicular impairment and progression of hair loss [8,9]. Therefore, effective prevention or management of AGA requires therapeutic strategies that reduce androgen-related signaling while simultaneously improving hair-growth-promoting factors within the hair follicle microenvironment.

Currently, the U.S. Food and Drug Administration has approved only two pharmacological treatments for AGA, viz., finasteride (FN) and minoxidil (MXD). The former reduces DHT levels by inhibiting 5α-reductase activity [10], whereas the latter is believed to promote hair growth partially through vasodilatory and growth factor-related effects [11]. Nevertheless, both agents are associated with adverse effects, including sexual dysfunction with FN and local scalp irritation with MXD [4,10–12], emphasizing the need for safer and more effective therapeutic strategies for AGA.

Consequently, natural compounds have attracted increasing interest as alternative therapeutic candidates for alopecia, particularly considering the limitations and adverse effects associated with current pharmacological treatments.

In this regard, *Sinomenium acutum* (Thunb.) Rehd. et Wils. (SA), as a woody climbing vine of the family Menispermaceae, has long been used in traditional Chinese medicine, particularly for the treatment of rheumatism, arthralgia, and other pain- and inflammation-related conditions. SA has also been reported to exhibit diverse biological activities, including antioxidant, anti-inflammatory, antitumor, and hepatoprotective effects [13]. However, to our knowledge, there is no documented traditional use of *S. acutum* specifically for the treatment of hair loss or alopecia. Nevertheless, its reported antioxidant and anti-inflammatory activities provided a pharmacological rationale for investigating its potential effects on hair growth. Furthermore, several bioactive compounds have been isolated from SA, such as sinomenine (SIN), magnoflorine, acutumine, and N-feruloyltyramine, among which SIN is considered the major active constituent [14]. Sinomenine has been widely used for treating autoimmune diseases, particularly rheumatoid arthritis [15], and also exerts protective effects in various disease models, including diabetic nephropathy, arrhythmia, urinary protein abnormalities, and brain tissue injury [16]. Studies have also reported its antioxidant and anti-inflammatory activities, including the suppression of proinflammatory cytokines, and its protective effects against lipopolysaccharide (LPS)-induced liver injury [17,18].

Despite these diverse biological activities of SIN, there have been no studies on the effects of SA and SIN on hair growth. Therefore, this study investigated the hair-growth-

promoting potential of SA rhizome extract (SAE) and its major constituent, SIN, using human dermal papilla cells (HDPCs) and a mouse model.

2. Materials and Methods

2.1. Preparation of SAE and Quantification of SIN

The rhizomes of *S. acutum* (SA) were obtained from Kyungdong Oriental Herbal Market in Seoul, South Korea (January 2018. The specimen (voucher no. HYUP-SA-001) was preserved in the Herbarium of the College of Pharmacy, Hanyang University. For extraction, 1.5 kg of pulverized SA was refluxed thrice with 50% aqueous ethanol for 2 h each time. After filtering and pooling the extract solutions, the solvent was removed under diminished pressure via rotary evaporation, which produced 221.4 g of dry crude extract (SAE).

Sinomenine (SIN) used in the biological experiments was isolated and purified from *S. acutum* in the laboratory of Prof. Chul Young Kim according to a previously reported procedure. The isolation and structural characterization of SIN, including NMR and ESI-MS analyses, have been described previously [19,20].

For chemical characterization of SAE, sinomenine (SIN) was selected as a specific marker compound and quantified by HPLC. Chromatographic separation of the crude extract was carried out on a Hector C18 column (4.6 × 250 mm, 5 µm; RStech Corp.,Daejeon, Republic of Korea). The mobile phase was composed of 0.1% (*v*/*v*) formic acid in acetonitrile (solvent A) and 0.1% (*v*/*v*) formic acid in water (solvent B), applied under the following gradient program: 5% A at 0 min, 8% A at 5 min, 10% A at 15 min, 20% A at 25 min, 80% A at 30 min, and 90% A at 40 min. Operating parameters were set as follows: a column temperature of 40 °C, a flow rate of 1.0 mL/min, a detection wavelength of 280 nm, and an injection volume of 10 µL. For quantitative analysis, three SAE samples were dissolved in methanol at a concentration of 1.5 mg/mL. Sinomenine was prepared in methanol at 1 mg/mL and serially diluted to 0.2, 0.1, 0.05, 0.025, and 0.0125 mg/mL to construct an external calibration curve. The SIN content in SAE was calculated from the calibration curve and determined to be 21.7 mg/g. The HPLC chromatogram of SAE showing the characteristic SIN peak is presented in Figure 1. Both SAE and SIN stocks were dissolved in growth medium for in vitro experiments and in distilled water (DW) for in vivo experiments.

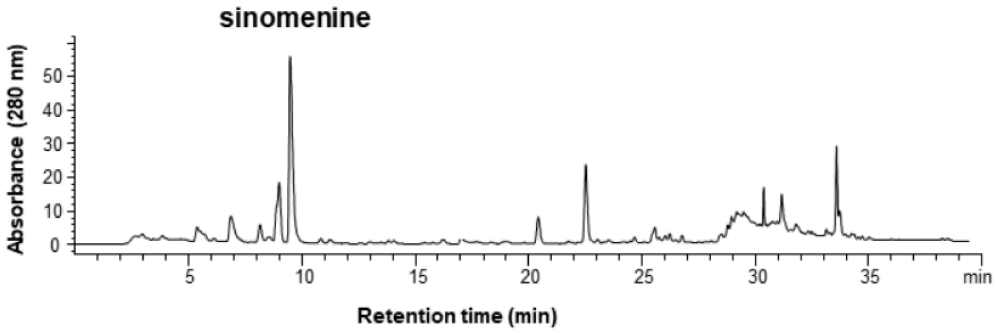


Figure 1. HPLC chromatogram of *Sinomenium acutum* rhizome extract (SAE) showing the characteristic sinomenine (SIN) peak.

2.2. Antiradical Activity

The scavenging capacity against free radicals was evaluated using 2,2-diphenyl-1-picrylhydrazyl (DPPH) and 2,2-azino-bis (3-ethylbenzothiazoline-6-sulfonic acid) (ABTS), both procured from Sigma-Aldrich (St. Louis, MO, USA). For the assay, the test sample dissolved in DMSO (1 mg/mL) was combined with a methanolic DPPH solution at a

volumetric ratio of 1:4 [21]. The final concentrations of SAE were 31.25, 62.5, 125, and 200 μg/mL, and those of SIN were 0.33, 0.66, 1.32, and 3.29 μg/mL (1, 2, 4, and 10 μM, respectively). The absorbance of the ABTS solution was diluted to ~0.7. Samples were measured at 517 nm for the DPPH assay and at 734 nm for the ABTS assay using a microplate reader (PerkinElmer, Inc., Waltham, MA, USA). The half-maximal inhibitory concentration (IC_{50}) was defined as the concentration required to inhibit 50% of radical activity, with lower IC_{50} values indicating higher radical-scavenging capacity.

2.3. Animal Experimental Design

Male C57BL/6 mice (aged 6 weeks) were purchased from Central Lab Animal Inc. (Seoul, Republic of Korea). Male mice were used to minimize variability associated with sex-hormone-dependent regulation of the hair cycle [22,23]. All animals were housed under controlled conditions (23 ± 2 °C, 12 h light/dark cycle) with free access to standard chow and water. The study protocol was approved by the Institutional Animal Care and Use Committee of Eulji University (EUIACUC-24-07, 30 July 2024) and the experiments were conducted in accordance with the ARRIVE guidelines.

This study employed a randomized controlled design with body weight-based stratification, in which the individual animal served as the experimental unit. After a 1-week acclimatization period, 32 mice (7 weeks of age; baseline body weights, 20–24 g) were randomly allocated into four groups (n = 8 per group)—control (treated with DW), 3% MXD, 0.5% SAE, and 0.5% SIN—using simple random assignment with stratification by body weight to ensure a balanced baseline distribution across groups. Group allocation was concealed from the investigators responsible for outcome assessment, and all outcome measurements were performed by an investigator blinded to treatment assignment. The sample size was determined based on previous depilation-induced hair regrowth studies in C57BL/6 mice employing comparable group sizes, which have been shown to provide sufficient statistical power to detect treatment-related differences in hair regrowth parameters [24]. The 0.5% concentration was selected based on previously reported effective topical concentration ranges (0.01–1%) for hair-growth agents in clinical and animal studies [25–27], rather than through formal dose optimization in the present animal model.

The dorsal skin of each mouse was shaved using an electric clipper, followed by the application of a depilatory cream (VEET, Massy, France) to synchronize the hair cycle to the telogen phase [28,29]. Beginning 1 day after depilation, 0.5 mL of each treatment was applied once daily for 15 days to the entire dorsal skin using a brush and gently spread until fully absorbed. Distilled water (DW) was used as the vehicle for all groups. The 15-day treatment period was selected based on established depilation-induced hair regrowth models in C57BL/6 mice, in which anagen induction and early hair regrowth are commonly evaluated approximately 14–16 days after depilation [28,29]. General health and skin condition were monitored throughout the experimental period, and no abnormal health conditions or visible signs of skin irritation were observed. Exclusion criteria were established a priori: animals were excluded if they died during the experiment, exhibited body weight loss exceeding 20%, or showed signs of infection.

Photographs of the dorsal skin were captured on days 1, 3, 7, 10, 13, and 15. On day 15, the dorsal skin and hair samples were collected for histopathological analysis. Hair length was measured using a microscope, and dorsal skin pigmentation, used as an indirect indicator of anagen transition, was evaluated and scored as follows: 0 for 0%, 1 for 0–20%, 2 for 21–40%, 3 for 41–60%, 4 for 61–80%, and 5 for 81–100% pigmentation [30].

2.4. Immunohistochemistry

Dorsal skin samples were fixed in 4% formaldehyde for 24 h, embedded in paraffin, and sectioned longitudinally. Tissue morphology was evaluated using hematoxylin and eosin (H&E) staining. For histological quantification, 20 hair follicles per mouse were evaluated from H&E-stained dorsal skin sections (n = 8 mice per group). Hair follicles were classified as anagen or telogen based on their histological morphology according to established morphological criteria [31], and the anagen-to-telogen (A/T) ratio was calculated based on the numbers of anagen and telogen follicles. All slides were coded prior to evaluation, and assessment was performed by an investigator blinded to group allocation.

For immunohistochemistry, the paraffin sections were deparaffinized, rehydrated, and subjected to heat-induced antigen retrieval. After blocking, the sections were incubated overnight at 4 °C with an anti-VEGF primary antibody (1:1000; Santa Cruz Biotechnology, Dallas, TX, USA), followed by an HRP-conjugated secondary antibody. Signals were developed using DAB and counterstained with hematoxylin. The slides were then dehydrated, mounted, and examined under a light microscope.

2.5. Western Blot Analysis

Total proteins were isolated from dorsal skin samples utilizing CelLytic lysis buffer (Sigma-Aldrich, St. Louis, MO, USA) containing protease and phosphatase inhibitors. Following centrifugation at 23,000× g for 20 min at 4 °C, the resultant supernatants were harvested, and Bradford reagent was employed to quantify protein concentrations. Protein samples of equal quantities were resolved via 10–15% SDS-PAGE and subsequently electrotransferred onto PVDF membranes. The membranes were blocked using 3% skim milk, probed overnight with specific primary antibodies at 4 °C, and then treated with secondary antibodies conjugated to HRP. Immunoreactive bands were visualized using enhanced chemiluminescence (ECL) reagents on a chemiluminescence imaging system (ATTO, Daejeon, Republic of Korea). Primary antibodies targeting VEGF and TGF-β1 were purchased from Santa Cruz Biotechnology (Dallas, TX, USA), while those against bFGF, beta-catenin, and COX-2 were obtained from Cell Signaling Technology (Danvers, MA, USA); all primary antibodies were diluted at 1:1000.

2.6. ELISA for TGF-β

The levels of transforming growth factor beta 1 (TGF-β1) in the dorsal skin protein lysates were measured using a commercial ELISA kit (Thermo Fisher Scientific Corporation, Waltham, MA, USA) following the protocol provided by the manufacturer. Protein concentrations were quantified via the Bradford assay using bovine serum albumin as a standard, which allowed the normalization of TGF-β1 levels relative to total protein content. These normalized values are presented as fold changes compared with the control group. Optical absorbance was recorded at 450 nm on a microplate reader (PerkinElmer, Inc., Waltham, MA, USA).

2.7. Cell Culture

Human dermal papilla cells (HDPCs, immortalized) were acquired from CEFO Bio (Seoul, Republic of Korea). These cells were maintained in a specialized Follicle Dermal Papilla Cell Growth Medium (PromoCell, Heidelberg, Germany) supplemented with 4% fetal calf serum, 0.4% bovine pituitary extract, recombinant human insulin at 5 μg/mL, and 1 ng/mL of basic fibroblast growth factor (bFGF). The growth medium was supplemented with 1% penicillin–streptomycin from Welgene (Daegu, Republic of Korea). The cell treatment conditions were as follows: HDPCs were seeded at a density of 1.0 × 10^6 cells/mL and allowed to attach for 24 h. A DHT concentration of 100 μM was selected based on a

previously established in vitro androgen-stimulated HDPC model using human dermal papilla cells [32]. Finasteride (FN) at 20 μM was used as a positive control based on concentrations employed in previous in vitro studies evaluating anti-androgenic activity [33]. Except for the untreated control group (CON), all experimental groups were exposed to 100 μM DHT (TCI, Tokyo, Japan) and cotreated with 20 μM FN (TCI, Tokyo, Japan), 100 μg/mL SAE, or SIN at concentrations of 50, 100, and 200 nM for 48 h.

2.8. Cell Viability Assay

The HDPCs were seeded in 96-well plates at a density of 1.0×10^4 cells/well and allowed to attach for 24 h, followed by treatment with SIN (1–500 nM) or SAE (1–500 μg/mL) for 48 h. Cell viability was determined using the MTT (Duchefa biochemie, Haarlem, The Netherlands) assay by incubating the cells with 1 mg/mL MTT for 2 h, followed by solubilization of formazan crystals with 2-propanol. Absorbance was then measured at 540 nm using a microplate reader (PerkinElmer, Inc., Waltham, MA, USA), and viability was expressed as a percentage of the untreated control. All experiments were conducted in triplicate.

2.9. Real-Time Quantitative PCR

Cells were plated into 6-well plates at a density of 1.0×10^6 cells/mL and incubated with either SAE or SIN for 24 h. Total cellular RNA was extracted using Trizol reagent, following which complementary DNA (cDNA) was synthesized utilizing the PrimerScript 1st strand cDNA Synthesis Kit (Takara BIO Inc., Shiga, Japan). Real-time quantitative PCR (RT-qPCR) was performed on an ABI real-time PCR system with SYBR Premix Ex Taq II ROX plus (Takara Bio Inc., Shiga, Japan) to evaluate mRNA expression levels. Detailed primer sequences are provided in Table 1. Target gene expression was quantified using the comparative $2^{-\Delta\Delta Ct}$ analytical method.

Table 1. Primer set sequences used for RT-qPCR analysis.

Primer	Forward	Reverse
GAPDH	TGTTGCCATCAATGACCCCTT	CTCCACGACGTACTCAGCG
VEGF	GGAGGGCAGAATCATCACGA	GCTCATCTCTCCTATGTGCTGG
bFGF	CGGCTGTACTGCAAAAACGG	GATGTGAGGGTCGCTCTTCTCC
TGF-β1	ACAGCAACAATTCCTGGCGAT	AAAGCCCTCAATTTCCCCTCC
β-catenin	CATCTACACAGTTTGATGCTGCT	GCAGTTTTGTCAGTTCAGGGA
DKK-1	CCTTGAACTCGGTTCTCAATTCC	CAATGGTCTGGTACTTATTCCCG

2.10. Statistical Analysis

All data are expressed as the mean and standard deviation (SD). Statistical significance was analyzed using SPSS 20.0 software (IBM SPSS ver. 20.0.0 for Windows; IBM Co., Armonk, NY, USA). Significant differences among the groups were analyzed using one-way ANOVA followed by Tukey's post hoc test. Statistical significance was set at $p < 0.05$.

2.11. Generative AI Statement

During the preparation of this work, the authors used Perplexity Pro version (Perplexity AI, Inc., San Francisco, CA, USA.) for the purpose of language editing, grammar polishing, and improving the readability of the manuscript. After using this tool, the authors reviewed and edited the content as needed and take full responsibility for the content of the publication.

3. Results

3.1. Antiradical Activity of SAE and SIN

Before evaluating its biological activity, HPLC analysis identified SIN as a characteristic marker peak of SAE (Figure 1). The radical-scavenging activities of SAE and SIN were determined using DPPH and ABTS radical-scavenging assays (Table 2). Overall, SIN demonstrated substantially stronger antiradical activity than SAE, as indicated by consistently lower IC_{50} values. In the DPPH assay, SIN exhibited an IC_{50} value of 15.17 μg/mL, whereas SAE demonstrated an IC_{50} value of 85.71 μg/mL, indicating that the former was ~5.7-fold more potent than the latter; similarly, in the ABTS assay, SIN displayed a lower IC_{50} value of 1.56 μg/mL compared with 4.14 μg/mL for SAE, corresponding to ~2.7-fold higher radical-scavenging activity.

Table 2. Antiradical activities of SAE and SIN determined by DPPH and ABTS radical-scavenging assays.

Sample	DPPH (IC_{50})	ABTS (IC_{50})
SAE (μg/mL)	85.71 ± 2.12	4.14 ± 0.03
SIN (μg/mL)	15.17 ± 2.33	1.56 ± 0.00
Ascorbic acid (μg/mL)	63.47 ± 1.28	3.00 ± 0.57

DPPH and ABTS radical-scavenging activities are expressed as IC_{50} values. Ascorbic acid was used as a positive control. Data are presented as mean ± SD (n = 4).

3.2. Effects of SAE and SIN on Hair Regrowth in Mouse Dorsal Skin

The hair-regenerative activities of SAE and SIN were evaluated by conducting an in vivo experiment for 15 days. As depicted in Figure 2A, the bright pink dorsal skin observed in all mice on day 1 of treatment suggested that the hair cycle was synchronized with the telogen phase. On day 10, the untreated control group maintained its characteristic bright pink dorsal skin, indicating a continuation of the telogen phase. However, the MXD-, SAE-, and SIN-treated groups showed a darker gray pigmentation, suggesting a transition from the telogen to the anagen phase. On day 15, when all mice were sacrificed, most of the dorsal skin areas appeared black, suggesting progression into the anagen phase; nevertheless, the hair growth of most mice in the CON group remained in the telogen phase. Analysis of hair shaft length showed that SAE treatment significantly increased the hair length by ~1.6-fold compared with that in the untreated control (CON) group ($p < 0.05$). Remarkably, SIN exerted a markedly stronger effect, extending the hair length by >2.2-fold compared with that in the CON group ($p < 0.001$). Furthermore, the hair-growth-promoting efficacy of SIN was comparable to that of MXD, whereas SAE resulted in only a moderate increase in hair shaft elongation (Figure 2B). Anagen transition was also assessed using a dorsal skin pigmentation-based scoring system, as illustrated in Figure 2C. The CON group maintained low pigmentation scores during the early experimental period, whereas the MXD, SAE, and SIN groups showed significantly increased scores, consistent with earlier anagen transition. In particular, the SIN group exhibited the most remarkable improvement, with a greater proportion of animals achieving high scores (4–5) by the end of the experiment. Importantly, SIN exerted statistically significant effects ($p < 0.01$ vs. CON) comparable to those exerted by MXD, whereas SAE induced only a moderate increase compared with that in the CON group.

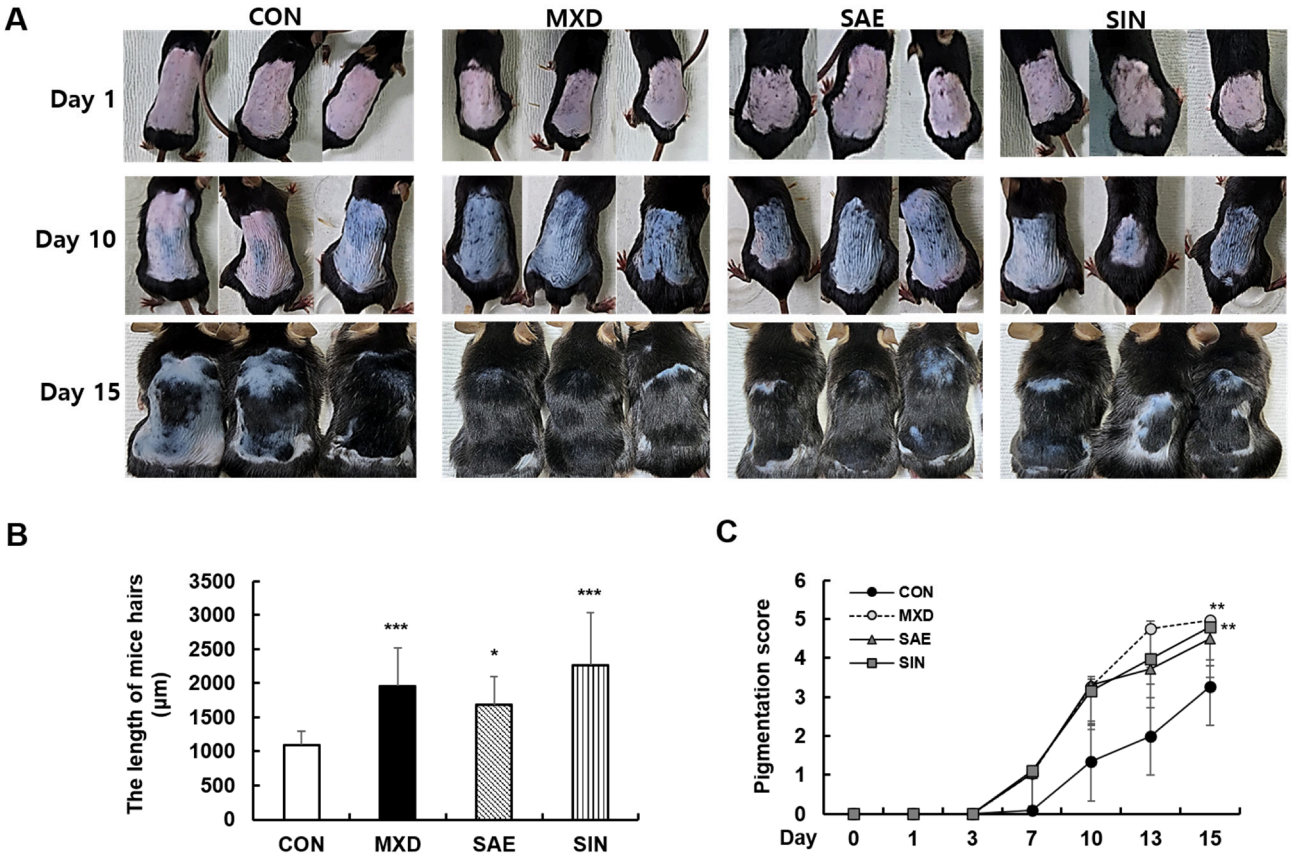


Figure 2. Effects of SAE and SIN on hair regrowth in mouse dorsal skin. (**A**) Each group was treated with DW, 3% MXD, 0.5% SAE, or 0.5% SIN for 15 days. Representative photographs of three mice per group are shown for days 1, 10, and 15. (**B**) Hair length was measured on day 15. (**C**) Dorsal skin pigmentation scores, used as an indirect indicator of anagen transition, were evaluated as described in the Materials and Methods. Quantitative data in (**B**,**C**) are expressed as mean ± SD (n = 8 mice per group). * $p < 0.05$, ** $p < 0.01$, and *** $p < 0.001$ vs. CON. CON, distilled water-treated control; MXD, 3% minoxidil; SAE, 0.5% *Sinomenium acutum* rhizome extract; SIN, 0.5% sinomenine.

3.3. Effects of SAE and SIN on Hair Follicle Growth in Mouse Dorsal Skin

Histological examination was conducted using H&E staining to evaluate the hair-follicle-growth-promoting activity of SAE and SIN using the dorsal skin samples collected from mice. The control group exhibited a delayed entry into the anagen phase compared with the other groups; most hair follicles in the control group were located beneath the epidermis, and their density was significantly lower than that in the treatment groups. In contrast, the MXD group demonstrated active hair follicle growth, with hair follicles rooted deep in the subcutaneous tissue. The SAE and SIN groups exhibited histological characteristics similar to those of the MXD group. The hair follicles of mice treated with SAE displayed an elongated structure typical of the anagen phase. Remarkably, the SAE and SIN groups exhibited longer dermal length than the positive control group, indicating that more hair follicles were located in the deep region (Figure 3A). The A/T ratio graph (Figure 3B,C) quantifies the number of hair follicles in the anagen and telogen phases. When the control group (CON) was normalized to 1 and the other groups were compared with CON, the A/T ratios of all treatment groups were significantly higher at >2-fold ($p < 0.001$) that of CON.

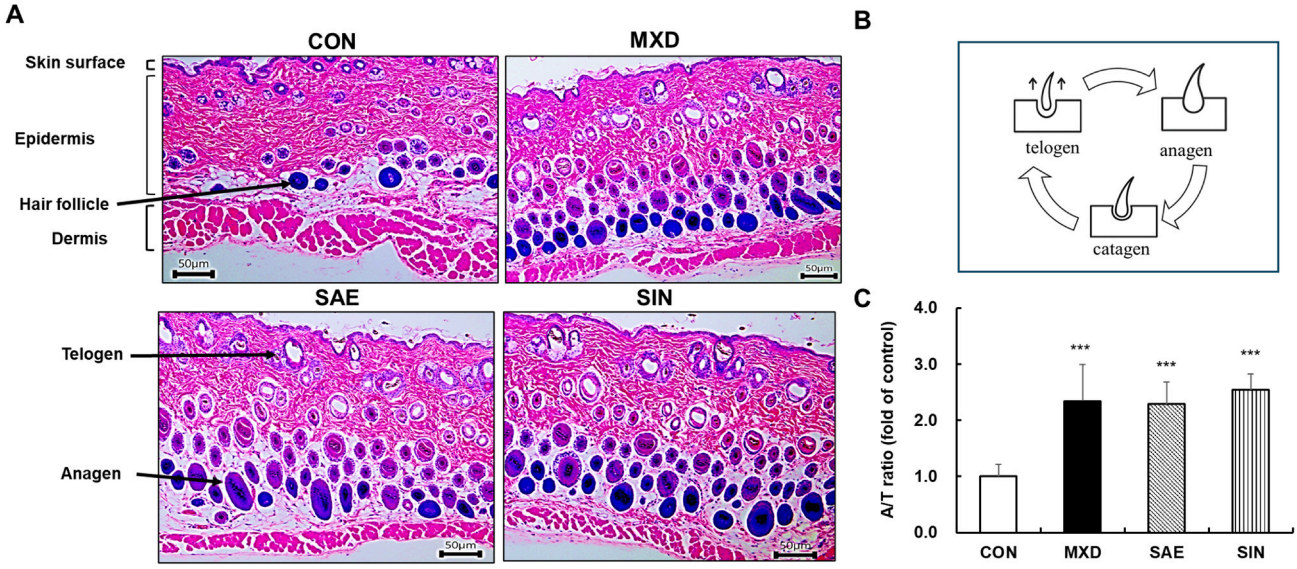


Figure 3. Effects of SAE and SIN on hair follicle cycle progression in mouse dorsal skin. (**A**) Representative H&E-stained cross-sections of dorsal skin from mice treated daily for 15 days with distilled water (CON), 3% minoxidil (MXD), 0.5% *Sinomenium acutum* rhizome extract (SAE), or 0.5% sinomenine (SIN). Scale bar = 50 μm. (**B**) Normal hair cycle. The anagen phase is a hair-growth period, the catagen phase is a short period lasting 1–2 weeks, and the telogen phase indicates the cessation of hair growth, entering a resting state. The arrows indicate the direction of progression through the hair cycle. (**C**) Quantification of the anagen-to-telogen (A/T) ratio expressed as fold change relative to CON. Data are expressed as mean ± SD (n = 8). *** $p < 0.001$ vs. CON. No significant differences were observed among the MXD, SAE, and SIN groups.

3.4. Effects of SAE and SIN on the Expression of VEGF and TGF-β1 in Mouse Dorsal Skin

Vascular endothelial growth factor (VEGF) plays a vital role in promoting angiogenesis and improving blood supply around hair follicles, which supports follicular growth and regeneration [34]. Conversely, TGF-β1 regulates the hair cycle by inducing catagen and follicular regression [35]. Therefore, we investigated the differential expression of these proteins between the control and treatment groups and found that VEGF immunoreactivity slightly increased in the MXD group compared with that in the CON group, as depicted in Figure 4A. In contrast, SAE markedly increased VEGF-positive staining, particularly in the epidermis, exhibiting stronger signals than those observed in the CON and MXD groups. Vascular endothelial growth factor staining was generally more prominent in dermal hair follicles than in the epidermis. Sinomenine treatment resulted in a similar pattern to that shown by SAE treatment, characterized by stronger epidermal VEGF expression and distinct foci of intense VEGF positivity. To further explore whether SAE and SIN modulate inhibitory signaling associated with hair-growth suppression, TGF-β1 levels were quantified in proteins extracted from dorsal skin tissues using ELISA (Figure 4B). Minoxidil ($p < 0.05$) significantly reduced TGF-β1 levels compared with those in CON, whereas SAE ($p < 0.001$) and SIN ($p < 0.001$) induced even greater reductions, decreasing TGF-β1 concentrations to approximately half of those in the CON group. Consistent with these observations, the Western blot analysis (Figure 4C,D) revealed >2-fold increased VEGF protein expression in the SIN ($p < 0.001$) group compared with that in the CON group. Minoxidil treatment also increased VEGF expression by ~1.6-fold ($p < 0.05$) compared with CON treatment. Moreover, SAE treatment induced an ~1.4-fold increase in VEGF expression, although this change did not reach statistical significance. Furthermore, TGF-β1 protein levels significantly decreased in all treatment groups compared with those in the CON group ($p < 0.01$), with the SAE and SIN groups exhibiting the most remarkable

inhibitory effects. Altogether, these results suggest that SAE and SIN promote the telogen-to-anagen transition in the mouse dorsal skin, accompanied by the upregulation of VEGF and the concomitant downregulation of TGF-β1.

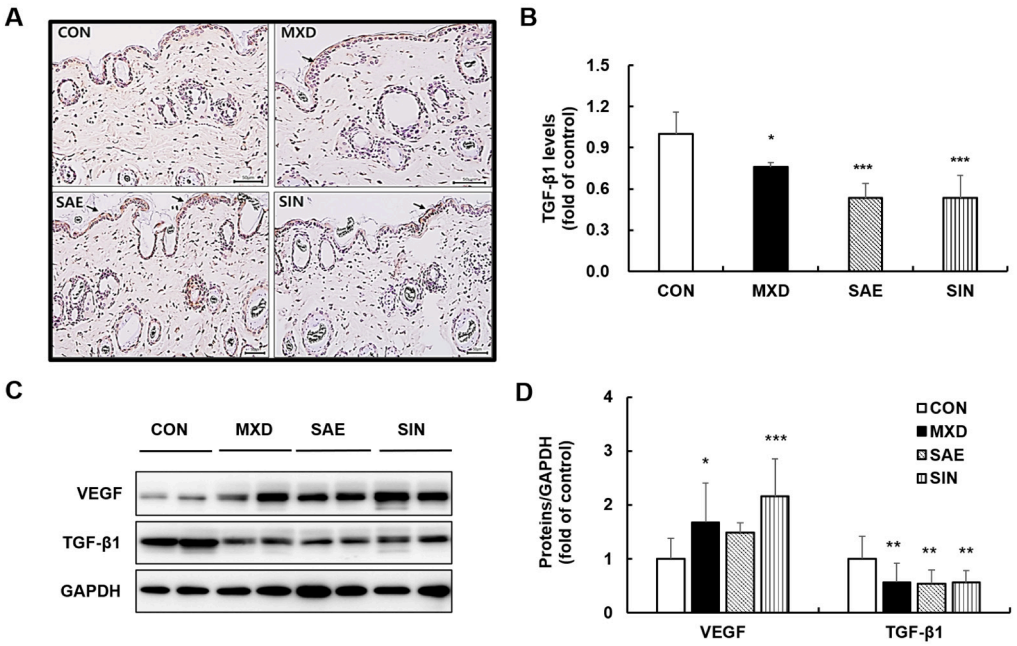


Figure 4. Effects of SAE and SIN on VEGF and TGF-β1 expression in mouse dorsal skin. (**A**) Representative immunohistochemical staining images of vascular endothelial growth factor (VEGF) in dorsal skin sections from mice treated with distilled water, 3% minoxidil (MXD), 0.5% *Sinomenium acutum* rhizome extract (SAE), or 0.5% sinomenine (SIN) for 15 days. Vascular endothelial growth factor (VEGF)-positive signals are indicated by brown staining (arrows). Scale bar = 50 μm. (**B**) Transforming growth factor beta 1 (TGF-β1) levels in the dorsal skin were measured by ELISA and expressed as fold change relative to CON. (**C**) Representative Western blot images depicting VEGF and TGF-β1 protein expression in dorsal skin tissues. GAPDH was used as a loading control. (**D**) Densitometric analysis of VEGF and TGF-β1 protein levels normalized to GAPDH and expressed as fold change relative to CON. Data are expressed as mean ± SD (n = 8). * $p < 0.05$, ** $p < 0.01$, and *** $p < 0.001$ vs. CON.

3.5. Effects of SAE and SIN on Cytotoxicity in HDPCs

To further examine the hair-promoting effect of SAE and SIN and the associated cellular changes, HDPCs were treated with or without various concentrations of SAE and SIN, and cell viability was measured using the MTT assay (Figure 5). Although SAE exhibited no significant cytotoxicity at low-to-intermediate concentrations, it reduced the viability of HDPCs at 200 and 500 μg/mL, indicating potential cytotoxicity at higher doses. Conversely, SIN exerted no effect on the viability of HDPCs across the tested concentration range (1–500 nM), thereby indicating that these concentrations were suitable. Accordingly, non-cytotoxic concentrations of SAE (100 μg/mL) and SIN (50, 100, and 200 nM) were used in all subsequent experiments. A formal efficacy-based dose optimization was not performed; rather, these concentrations were selected based on preliminary cytotoxicity screening. *Sinomenium acutum* rhizome extract at 100 μg/mL was selected as the highest non-cytotoxic concentration, whereas SIN at 50, 100, and 200 nM was chosen within the non-cytotoxic range to evaluate concentration-dependent effects. While a formal efficacy-based dose optimization was not performed, these ranges allowed for the evaluation of concentration-dependent effects at biologically relevant levels while avoiding cytotoxicity. Furthermore, these non-cytotoxic thresholds align with previous reports of SIN in cellular models [36], supporting the validity of the chosen experimental doses.

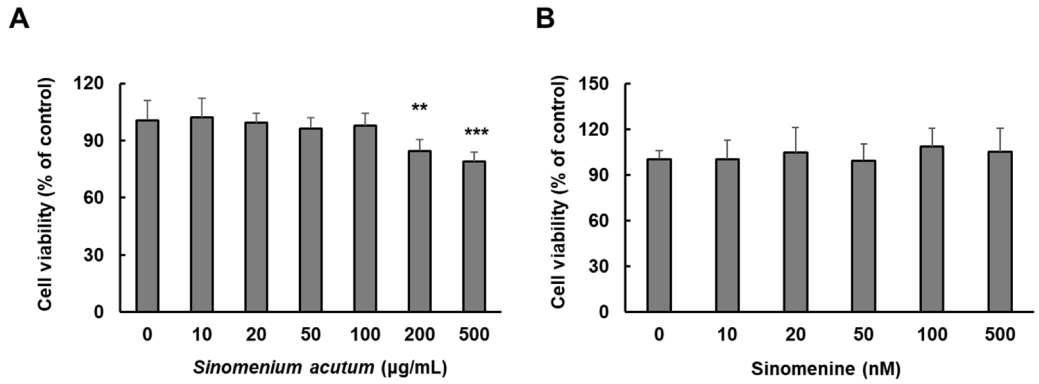


Figure 5. Effects of SAE and SIN on the viability of HDPCs. HDPCs were treated with (**A**) SAE (1–500 μg/mL) or (**B**) SIN (1–500 nM) for 48 h, and cell viability was evaluated using the MTT assay. Cell viability is expressed as a percentage of untreated control. Data are represented as mean ± SD (n = 4). ** $p < 0.01$ and *** $p < 0.001$ vs. untreated control.

3.6. Effects of SAE and SIN on Growth-Promoting Factors in DHT-Stimulated HDPCs

To explore the molecular changes associated with the hair-growth-promoting effects of SAE and SIN, we determined the expression of key hair-follicle-growth-related factors, VEGF and bFGF, in HDPCs treated with DHT. As depicted in Figure 6A, DHT treatment tended to suppress the mRNA levels of VEGF and bFGF compared with those in the untreated control (CON) group, although the reduction was not statistically significant. Remarkably, SAE treatment significantly increased the mRNA expression of VEGF and bFGF in the presence of DHT, and SIN similarly increased their expression in a dose-dependent manner, with more distinct effects at higher concentrations. Consistent with these findings, the protein expression analysis showed a similar pattern of upregulation by SAE and SIN (Figure 6B). Furthermore, Western blot and densitometric analyses revealed that both treatments increased the protein levels of VEGF and bFGF compared with DHT treatment, with SIN at 200 nM inducing the most robust increase (bFGF, $p < 0.05$). SIN exhibited stronger, dose-dependent induction of VEGF and bFGF protein expression, suggesting that it may contribute to the growth factor-promoting activity of SAE.

3.7. Effects of SAE and SIN on Wnt/β-Catenin-Related Markers in DHT-Stimulated HDPCs

To examine whether the effects of SAE and SIN were associated with Wnt/β-catenin signaling, we evaluated the expression of β-catenin and its antagonist dickkopf-1 (DKK-1) [8]. The positive control, FN, showed no significant alterations in β-catenin mRNA levels compared with the DHT-treated group; however, it showed ~0.7-fold ($p < 0.001$) reduced DKK-1 mRNA expression compared with that in the DHT-treated group. *Sinomenium acutum* rhizome extract markedly increased β-catenin expression while reducing DKK-1 expression; similarly, SIN increased β-catenin mRNA expression in a dose-dependent manner (1.2-, 1.4-, and 1.6-fold; $p < 0.01$) and proportionally reduced DKK-1 expression (0.8-, 0.7-, and 0.5-fold, respectively; Figure 7A,B). At the protein level, β-catenin expression showed no significant changes in the DHT-stimulated group. β-Catenin protein expression was evaluated as a marker associated with Wnt/β-catenin signaling in this study. Treatment with SAE significantly increased β-catenin protein expression by ~2.5-fold ($p < 0.01$), and sinomenine induced a concentration-dependent increase of approximately 1.1-, 1.6-, and 2.4-fold ($p < 0.05$), with the greatest increase observed at 200 nM among the concentrations tested (Figure 7C,D).

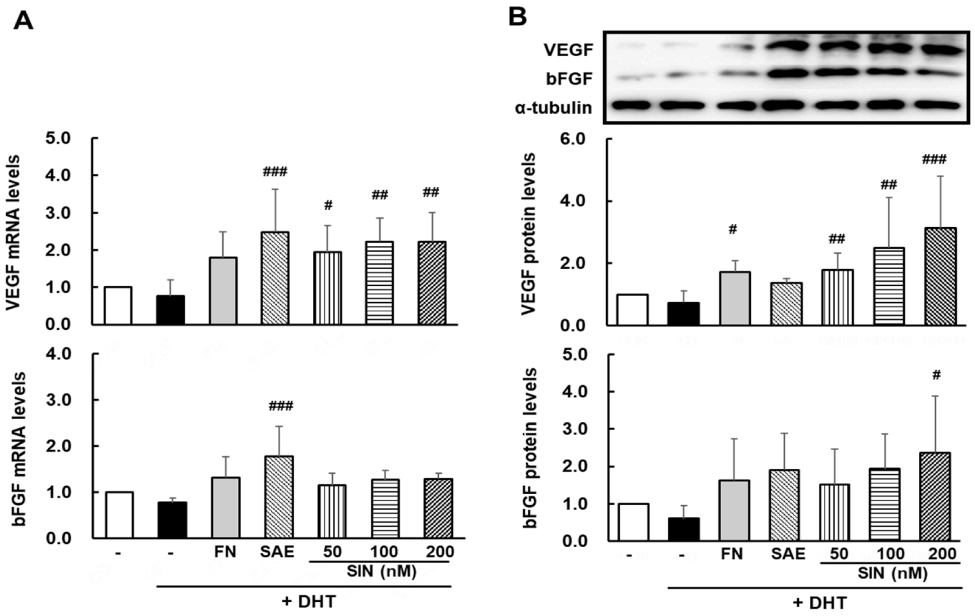


Figure 6. Effects of SAE and SIN on VEGF and bFGF expressions in DHT-stimulated HDPCs. HDPCs were stimulated with dihydrotestosterone (DHT) to model androgen-induced cellular stress and then treated with FN (20 μM), SAE (100 μg/mL), or SIN (50, 100, and 200 nM). (**A**) Relative mRNA expression levels of VEGF (upper) and bFGF (lower) were analyzed by RT-*q*PCR and expressed as fold change relative to untreated control (CON). (**B**) Representative Western blot images depicting VEGF and bFGF protein expression in HDPCs, with α-tubulin as a loading control. Densitometric quantification of VEGF and bFGF protein levels normalized to α-tubulin and expressed relative to CON. Data are expressed as mean ± SD (n = 3–5). $^{\#}$ $p < 0.05$, $^{\#\#}$ $p < 0.01$, and $^{\#\#\#}$ $p < 0.001$ vs. DHT-only treatment.

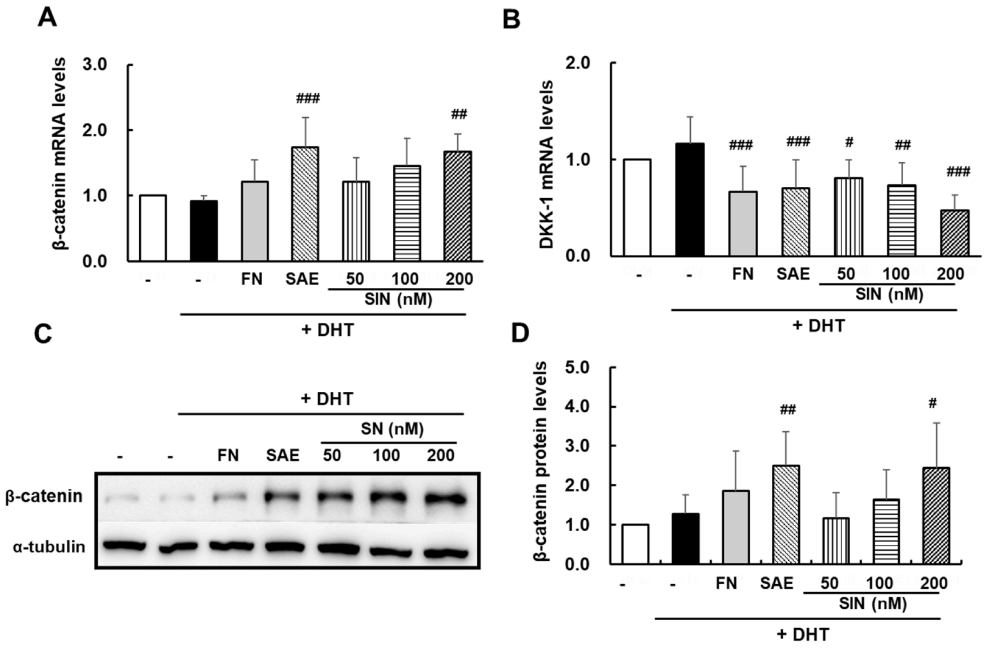


Figure 7. Effects of SAE and SIN on Wnt/β-catenin-related markers in DHT-stimulated HDPCs. (**A**,**B**) Relative mRNA expression levels of β-catenin and DKK-1 in DHT-stimulated HDPCs treated with FN (20 μM), SAE (100 μg/mL), or SIN (50, 100, and 200 nM). (**C**,**D**) Representative Western blot images and densitometric analysis of β-catenin protein expression under the same conditions, normalized to α-tubulin. Data are expressed as mean ± SD (n = 6). Statistical significance was determined compared with the DHT-stimulated group. $^{\#}$ $p < 0.05$, $^{\#\#}$ $p < 0.01$, and $^{\#\#\#}$ $p < 0.001$ vs. DHT-only treatment.

3.8. Effects of SAE and SIN on Inflammatory Response in DHT-Stimulated HDPCs

To evaluate the inflammatory response to SAE and SIN, we measured the expression of the proinflammatory cytokines IL-1β and IL-6 and the inflammatory mediator COX-2 in DHT-stimulated HDPCs. As depicted in Figure 8A,B, DHT stimulation significantly upregulated the mRNA expression of the inflammatory mediators IL-1β and IL-6, whereas SAE treatment markedly suppressed their expression and SIN treatment similarly reduced their levels in a concentration-dependent manner. Consistent with these findings, the Western blot analysis revealed that COX-2 protein levels, which are induced by these proinflammatory cytokines, were significantly downregulated by SAE and further decreased by SIN in a dose-dependent manner compared with those in the DHT-stimulated group (Figure 8C,D).

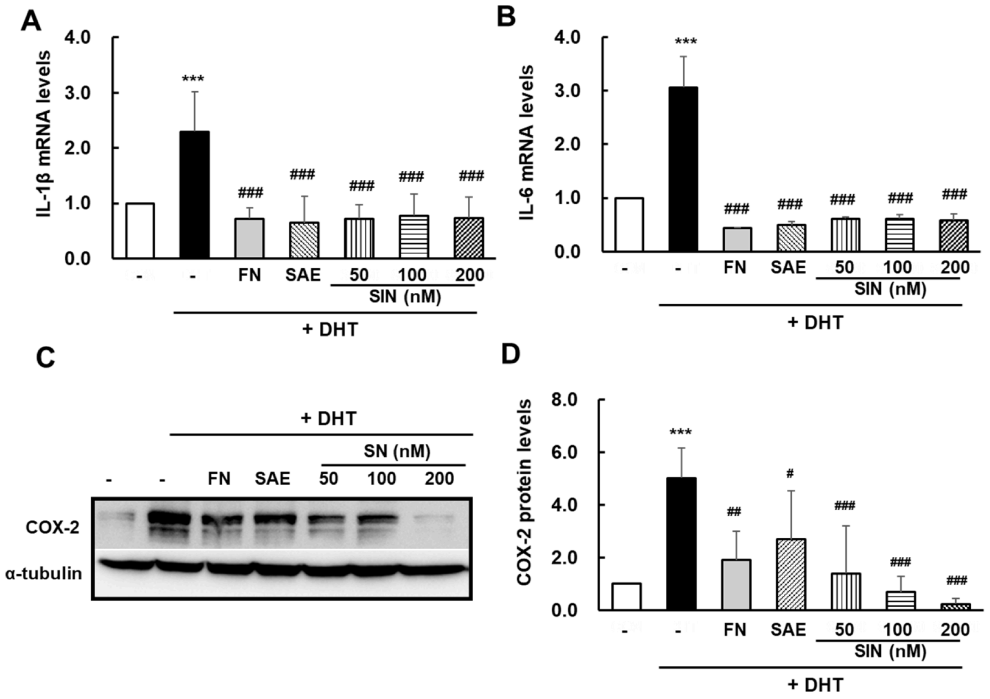


Figure 8. mRNA and protein expression of inflammatory cytokines and COX-2 protein levels in DHT-treated HDPCs. (**A**,**B**) Relative mRNA expression levels of proinflammatory mediators (IL-1β and IL-6) in DHT-stimulated HDPCs treated with FN (20 μM), SAE (100 μg/mL), or SIN (50, 100, and 200 nM). (**C**,**D**) Representative Western blot images and densitometric analysis of COX-2 protein expression under the same conditions, normalized to the loading control. All data are expressed as fold changes relative to untreated control. Data are represented as mean ± SD ($n = 4$). *** $p < 0.001$ vs. untreated control. $^{\#}$ $p < 0.05$, $^{\#\#}$ $p < 0.01$, and $^{\#\#\#}$ $p < 0.001$ vs. DHT-only treatment.

4. Discussion

This study showed that SAE and SIN promoted the telogen-to-anagen transition in a depilation-induced C57BL/6 mouse model and attenuated DHT-induced changes in growth factor, Wnt/β-catenin-related, and inflammatory markers in HDPCs. Various factors, including genetic predisposition, oxidative stress, mitochondrial dysfunction, and inflammatory responses, contribute to the regulation of hair loss. Considering that the anti-inflammatory effects of SIN are well established, we hypothesized that SIN derived from SAE could exert beneficial effects on hair loss and therefore designed experiments to test this possibility.

Sinomenine is a morphinan-type isoquinoline alkaloid [18,37] bearing a hydroxyl group at C-4 adjacent to a methoxy group at C-3 of ring A. This *o*-methoxyphenol (guaiacyl) motif is a well-recognized antioxidant pharmacophore, in which the phenolic hydroxyl

donates a hydrogen atom or electron to radical species and the resulting phenoxyl radical is stabilized by the adjacent methoxy group [38]. Consistent with this structural feature, direct comparison of the radical-scavenging activities revealed that SIN exhibited approximately 5.7- and 2.7-fold lower IC_{50} values than SAE in the DPPH and ABTS assays, respectively, on a mass basis, indicating correspondingly greater radical-scavenging activity, although structure-activity relationships were not directly examined in the present study. However, given that SIN accounts for only 2.17% (*w*/*w*) of SAE, a difference of approximately 46-fold would be expected if SIN were the sole antiradical constituent of the extract. The considerably smaller observed differences suggest that constituents other than SIN, which remain to be identified, also contribute to the overall radical-scavenging capacity of SAE as commonly observed in botanical extracts [37].

In the mouse model, topical application of SAE and SIN significantly promoted the telogen-to-anagen transition, thereby facilitating the initiation of hair regrowth. It should be noted that dorsal skin pigmentation is an indirect indicator of anagen transition rather than a direct measure of hair growth; therefore, the pigmentation findings were interpreted together with hair shaft length and histological assessment of hair follicles. The promotion of anagen transition may be associated with the observed upregulation of VEGF, which supports hair follicle vascularization and anagen maintenance, and downregulation of TGF-β1, which promotes catagen induction and follicular regression [39,40]. Consistent with this interpretation, Jang et al. reported that *Sargassum fusiforme* extract promoted hair regrowth in shaved C57BL/6 mice through regulation of VEGF/TGF-β signaling pathways [41].

Cytotoxicity evaluation showed that SAE did not significantly reduce HDPC viability at concentrations up to 100 μg/mL, whereas significant reductions were observed at higher concentrations of 200 and 500 μg/mL. In contrast, SIN did not significantly affect HDPC viability over the tested range of 1–500 nM. Accordingly, 100 μg/mL SAE and 50–200 nM SIN, concentrations that did not significantly reduce cell viability, were selected for subsequent mechanistic experiments. The margin between the effective and cytotoxicity-inducing concentrations of SAE was relatively narrow, with reduced HDPC viability observed at concentrations twofold above the effective concentration. Notably, SIN retained biological activity at low-nanomolar concentrations without affecting cell viability across the tested range, suggesting that the use of purified SIN or a SIN-enriched fraction may achieve comparable efficacy while avoiding the cytotoxicity associated with the crude extract. Fractionation to remove cytotoxic constituents, combined with compound-level activity profiling to delineate the relative contribution of individual constituents, as well as delivery approaches such as liposomal or nanoemulsion formulations that reduce the required applied concentration, may further improve this profile and warrant investigation in future studies. It should be emphasized, however, that these findings are limited to in vitro cytotoxicity in HDPCs and do not constitute evidence of cosmetic or topical safety; dedicated evaluations, including skin irritation, sensitization, and repeated-dose dermal toxicity testing, would be required prior to cosmetic application.

Based on the measured SIN content (21.7 mg/g), the 100 μg/mL SAE concentration used in cell experiments corresponds to a theoretical SIN concentration of approximately 6.6 μM, which is 33- to 132-fold higher than the purified SIN concentrations that elicited significant effects (50–200 nM). Based on its SIN content, SAE contained sufficient SIN on a molar basis to contribute substantially to its activity. However, because SAE contains multiple constituents and SIN-depleted extracts were not tested, the effects of SAE cannot be attributed exclusively to SIN.

The absence of a proportionally greater response to SAE suggests that the cellular effects had likely reached a plateau within this concentration range, and/or that the effective

availability of SIN is reduced within the complex extract matrix through interactions with co-occurring constituents. Notably, this pattern differs from that observed in the cell-free radical-scavenging assays, suggesting that the chemical antiradical capacity and the cellular activity of SAE may be driven by partly distinct constituents.

In the DHT-stimulated HDPCs, both SAE and SIN treatments increased expression of the growth factors VEGF and bFGF, which are crucial for the proliferation of dermal papilla cells and the elongation of hair shafts. Both bFGF and VEGF are well-recognized pro-growth factors involved in hair follicle regeneration: the latter promotes hair follicle angiogenesis and supports anagen maintenance by improving the activity of dermal papilla cells, whereas the former functions as a potent mitogenic factor that facilitates the proliferation of dermal papilla cells and the development of hair follicles [34,42]. Because DHT has been reported to suppress these factors in AGA [32], the concentration-dependent increase in VEGF and bFGF by SIN supports further evaluation of SIN in androgen-related hair loss models.

Wnt/β-catenin signaling is essential for anagen induction and hair follicle regeneration; however, it is negatively regulated by DKK-1 [43], which is associated with anagen-to-telogen transition and inhibition of hair growth. Therefore, the coordinated regulation of pro-growth factors (VEGF and bFGF) and inhibitory mediators (TGF-β1 and DKK-1) may critically determine hair follicle cycling and hair regrowth outcomes [44,45]. In the present study, SIN increased β-catenin expression and decreased DKK-1 expression in a concentration-dependent manner across 50, 100, and 200 nM, with the effect at 200 nM being significantly greater than that at 100 nM. The concurrent decrease in DKK-1 and increase in β-catenin are consistent with, but do not demonstrate, enhanced Wnt/β-catenin signaling. As 200 nM represented the highest concentration tested and the response had not clearly plateaued, the maximal effective concentration of SIN remains to be determined in future concentration–response studies. Notably, whereas finasteride (positive control) primarily suppressed DKK-1 expression without altering β-catenin mRNA expression, SAE and SIN exerted dual effects, suggesting that they may modulate Wnt/β-catenin-related signaling, which plays a central role in hair follicle stem cell activation and the telogen-to-anagen transition [46]. However, expression analysis alone cannot establish direct pathway activation, and the present findings should therefore be interpreted as suggestive, rather than confirmatory, of Wnt/β-catenin pathway involvement. Functional validation through pharmacological inhibition of the Wnt/β-catenin pathway (e.g., XAV939, ICG-001), TCF/LEF-based reporter assays, β-catenin knockdown, or quantification of canonical downstream target genes such as Axin2, Lef1, and Cyclin D1 will be required in future studies to conclusively establish a causal contribution of this pathway to the hair-growth-promoting effects of SAE and SIN. Therefore, the modulation of VEGF and TGF-β1 expression in the animal model and the changes in Wnt/β-catenin-related markers in HDPCs are associated with the hair-growth-promoting effects observed in this study.

Several studies have emphasized that inflammatory pathways are critically involved in the pathogenesis of hair loss, with proinflammatory cytokines such as IL-1β, IL-6, TNF-α, and IFN-γ, as well as COX-2-mediated prostaglandin synthesis, contributing to hair follicle immune privilege collapse, perifollicular microinflammation, and premature follicular regression [44]. In alopecia areata and AGA, these mediators promote T-cell and macrophage infiltration around the follicle, disrupt the hair cycle, and drive miniaturization, indicating that targeting inflammation is a rational strategy for hair loss intervention [47,48]. In the present study, DHT-induced inflammation, characterized by increased IL-1β, IL-6, and COX-2 in HDPCs, was effectively attenuated by SAE and SIN. As these three mediators are all transcriptional targets of NF-κB, their coordinated downregulation suggests modulation of a shared upstream regulatory pathway rather than independent effects

on individual genes. Consistent with this interpretation, SIN has been reported to suppress proinflammatory mediator production by inhibiting NF-κB and MAPK signaling, including upregulation of IκB and interference with NF-κB activation, in several cell types including keratinocytes [49]. Inhibition of NF-κB-dependent transcription therefore may represent a plausible mechanism underlying the anti-inflammatory effects observed here. Because reactive oxygen species also act as upstream activators of NF-κB signaling, the radical-scavenging capacity of SAE and SIN could conceivably contribute to this response. However, the DPPH and ABTS assays employed in this study are cell-free chemical assays that assess intrinsic radical-scavenging capacity and do not directly reflect intracellular antioxidant activity or downstream biological responses. The radical-scavenging activity of SAE and SIN and their suppression of IL-1β, IL-6, and COX-2 expression should therefore be interpreted as related but mechanistically distinct findings. Further investigations measuring intracellular ROS levels and assessing redox-sensitive signaling pathways, including IκB degradation, p65 nuclear translocation, MAPK phosphorylation, and Nrf2/HO-1 activation, are warranted to clarify whether the antioxidant and anti-inflammatory activities of SAE and SIN are causally linked.

Several limitations of this study should be acknowledged. First, the depilation-induced C57BL/6 model primarily reflects synchronized anagen induction rather than the androgen-driven progressive follicular miniaturization characteristic of human AGA. The present findings therefore support the hair regeneration potential of SAE and SIN but do not demonstrate therapeutic efficacy for AGA, which would require androgen-dependent models and clinical evaluation. Second, the single-dose design precludes formal dose–response characterization in vivo; however, the 0.5% concentration was selected within previously reported effective topical ranges [25,26] and future studies should evaluate dose-dependent effects across a broader concentration range. Third, the 15-day observation period was selected based on well-established depilation-induced C57BL/6 mouse models, in which synchronized anagen induction and visible hair regrowth are typically evaluated within approximately two weeks after depilation [50]. However, this short-term design does not encompass the subsequent catagen and telogen phases of the hair cycle. Consequently, it remains unclear whether the anagen-inducing effects of SAE and SIN translate into a prolonged anagen phase or an altered timing of catagen entry. Because some hair-growth promoters have been reported to cause rebound hair loss after treatment cessation [51,52], monitoring across at least one complete hair cycle will be necessary to verify the durability of these effects. Further studies incorporating extended longitudinal follow-up, together with repeated-dose toxicity assessments, are warranted to confirm the durability and safety profile of the observed effects. Fourth, SAE was standardized based on its major bioactive constituent, sinomenine (21.7 mg/g), which characterized the chemical composition of the extract used throughout the experiments. However, non-specific physicochemical parameters, such as moisture content, total ash, and extractive values, were not determined, and comprehensive physicochemical characterization according to pharmacopeial guidelines would be required for further standardization of SAE as a functional ingredient. Furthermore, although SIN is a major constituent of SAE, other constituents may also contribute to the observed effects. *Sinomenium acutum* is well-documented to contain a diverse array of other benzylisoquinoline alkaloids (such as acutumine and magnoflorine), as well as various phenolics, flavonoids, and triterpenoids [13,17]. The overall activity of SAE may therefore reflect the combined effects of multiple constituents. Bioassay-guided fractionation and comparison with SIN-depleted extracts will be required to clarify the contribution of each constituent. Fifth, immortalized HDPCs were used in this study. Although these cells provide reproducible results, they may differ from primary human dermal papilla cells in proliferation, androgen responsiveness, and hair-inductive properties. Therefore,

the in vitro findings should be confirmed using primary HDPCs or human hair follicle organ culture.

In addition to these limitations, several issues remain to be addressed before SAE and SIN can be applied in cosmetic formulations. Because skin and follicular penetration of SAE and SIN were not assessed, the effective concentrations observed in HDPCs cannot be directly related to the applied topical concentration, and human-relevant concentrations remain to be established. To bridge the gap between in vitro efficacy and in vivo delivery, optimizing cosmetic vehicles—such as utilizing liposomes, ethosomes, or nanoemulsions—will be essential to enhance the transdermal delivery and follicular targeting of these compounds into the human scalp. Further studies are therefore needed to characterize their penetration into the scalp and hair follicles, optimize their formulation, solubility, and stability, and assess irritation, sensitization and long-term safety. In addition, the relevance of the DHT-treated HDPC model to human AGA should be further examined using models that directly reflect androgen metabolism, including 5α-reductase activity.

5. Conclusions

Sinomenine, a major compound of SAE, showed radical-scavenging activity and promoted the telogen-to-anagen transition in mice; it increased the expression of hair-growth-promoting factors, including VEGF and bFGF, and suppressed the expression of inhibitory mediators such as TGF-β1, DKK-1, and proinflammatory cytokines. These regulatory effects were accompanied by alterations in key components of Wnt/β-catenin-related signaling, presenting it as an associated, rather than a confirmed mechanism (Figure 9). Altogether, these results suggest that the anagen-inducing and cycle-regulating activities of SAE may be partially attributable to SIN, indicating that SIN is a promising bioactive compound for hair care applications. Further validation, including functional mechanistic studies, long-term and androgen-dependent models, topical safety evaluation, and clinical studies, is required before its application as a hair-growth ingredient can be established.

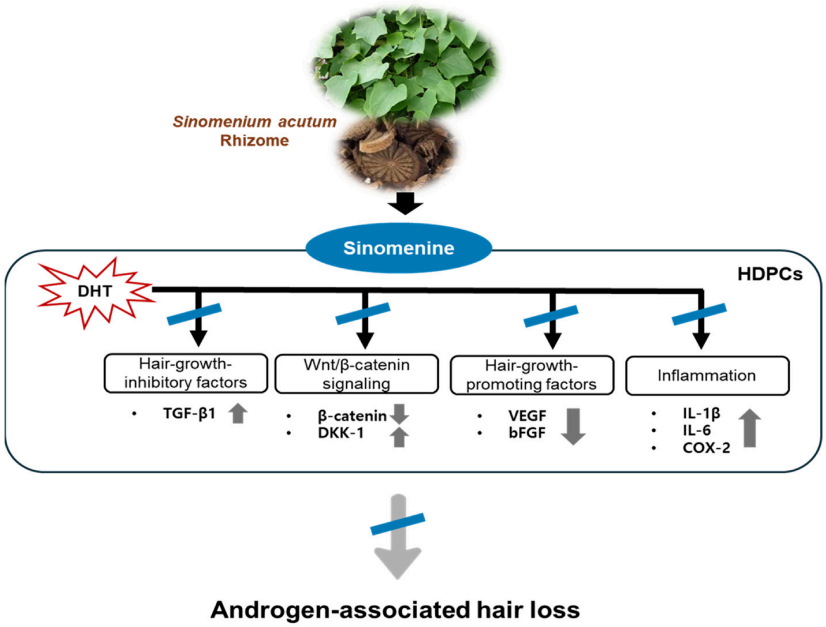


Figure 9. Schematic summary of the molecular changes associated with SIN in DHT-treated HDPCs. DHT increased hair-growth-inhibitory factors (TGF-β1) and inflammatory mediators (IL-1β, IL-6, and COX-2), and decreased Wnt/β-catenin-related markers and hair-growth-promoting factors (VEGF and bFGF). Gray arrows indicate DHT-induced changes; blue bars indicate attenuation by sinomenine. The pathways are shown in parallel and do not imply causal relationships.

Author Contributions: Conceptualization, C.E.K.; methodology, K.K., C.-H.L., E.-Y.P. and C.Y.K.; data curation, C.E.K., K.K., C.-H.L., E.-Y.P. and C.Y.K.; writing—original draft preparation, C.E.K. and K.K.; writing—review and editing, C.E.K., K.K., C.-H.L., E.-Y.P., C.Y.K. and Y.S.O.; supervision, Y.S.O.; funding acquisition, Y.S.O. All authors have read and agreed to the published version of the manuscript.

Funding: This study was supported by the Basic Science Research Program Grant (NRF-RS-2024-00336513) provided by the National Research Foundation of Korea (NRF), which is funded by the Ministry of Science, ICT and Future Planning.

Institutional Review Board Statement: The animal study protocol was approved by Institution Animal Care and Use Committee at Eulji University (protocol code EUIACUC-24-07; approval date: 30 July 2024) and conducted in accordance with the International Ethical Guidelines for Biomedical Research Involving Laboratory Animals and the ARRIVE 2.0 guidelines.

Informed Consent Statement: Not applicable.

Data Availability Statement: The data presented in this study are available from the corresponding author upon reasonable request.

Conflicts of Interest: The authors declare no conflicts of interest.

Abbreviations

A/T	Anagen-to-telogen ratio
AGA	Androgenetic alopecia
bFGF	Basic fibroblast growth factor
DHT	Dihydrotestosterone
DKK-1	Dickkopf-1
FN	Finasteride
HDPCs	Human dermal papilla cells
LPS	Lipopolysaccharide
MXD	Minoxidil
SAE	*Sinomenium acutum* rhizome extract
SIN	Sinomenine
TGF-β1	Transforming growth factor beta 1
TNF-α	Tumor necrosis factor alpha
VEGF	Vascular endothelial growth factor

References

1. Choi, J.Y.; Boo, M.Y.; Boo, Y.C. Can plant extracts help prevent hair loss or promote hair growth? A review comparing their therapeutic efficacies, phytochemical components, and modulatory targets. *Molecules* **2024**, *29*, 2288. [CrossRef] [PubMed]
2. Aukerman, E.L.; Jafferany, M. The psychological consequences of androgenetic alopecia: A systematic review. *J. Cosmet. Dermatol.* **2023**, *22*, 89–95. [CrossRef] [PubMed]
3. Nilforoushzadeh, M.A.; Golparvaran, M.; Yekaninejad, M.S. Assessment of quality of life and self-esteem in male patients with androgenetic alopecia before and after hair transplantation. *J. Cosmet. Dermatol.* **2023**, *22*, 2283–2287. [CrossRef] [PubMed]
4. Tampucci, S.; Paganini, V.; Burgalassi, S.; Chetoni, P.; Monti, D. Nanostructured drug delivery systems for targeting 5-α-reductase inhibitors to the hair follicle. *Pharmaceutics* **2022**, *14*, 286. [CrossRef] [PubMed]
5. Kidangazhiathmana, A.; Santhosh, P. Pathogenesis of androgenetic alopecia. *Clin. Dermatol. Rev.* **2022**, *6*, 69–74. [CrossRef]
6. Woo, M.J.; Kang, H.Y.; Paik, S.J.; Choi, H.J.; Uddin, S.; Lee, S.; Kim, S.-Y.; Choi, S.; Jung, S.K. The In Vivo and In Vitro Effects of Terminalia bellirica (Gaertn.) Roxb. Fruit Extract on Testosterone-Induced Hair Loss. *J. Microbiol. Biotechnol.* **2023**, *33*, 1467. [CrossRef] [PubMed]
7. Sekhavat, H.; Bar Yehuda, S.; Asotra, S. Using the Mechanisms of Action Involved in the Pathogenesis of Androgenetic Alopecia to Treat Hair Loss. *Int. J. Mol. Sci.* **2025**, *26*, 10712. [CrossRef] [PubMed]
8. Shin, D.W. The Molecular Mechanism of Natural Products Activating Wnt/β-Catenin Signaling Pathway for Improving Hair Loss. *Life* **2022**, *12*, 1856. [CrossRef] [PubMed]

9. Chen, S.; Li, L.; Ding, W.; Zhu, Y.; Zhou, N. Androgenetic Alopecia: An Update on Pathogenesis and Pharmacological Treatment. *Drug Des. Dev. Ther.* **2025**, *19*, 7349–7363. [CrossRef] [PubMed]
10. Devjani, S.; Ezemma, O.; Kelley, K.J.; Stratton, E.; Senna, M. Androgenetic Alopecia: Therapy Update. *Drugs* **2023**, *83*, 701–715. [CrossRef] [PubMed]
11. Gupta, A.; Talukder, M.; Venkataraman, M.; Bamimore, M. Minoxidil: A comprehensive review. *J. Dermatol. Treat.* **2022**, *33*, 1896–1906. [CrossRef] [PubMed]
12. Diviccaro, S.; Melcangi, R.C.; Giatti, S. Post-finasteride syndrome: An emerging clinical problem. *Neurobiol. Stress* **2020**, *12*, 100209. [CrossRef] [PubMed]
13. Zhen, X.; Wei, W.; Liu, L.; Fu, J.; Wang, J.; Hao, Z.; Ogaji, O.D.; Du, K.; Chang, Y. Botany, ethnopharmacology, phytochemistry, pharmacological activities, toxicity, quality control, clinical application and novel preparations of Sinomenii Caulis: An updated review. *J. Ethnopharmacol.* **2026**, *368*, 121793. [CrossRef] [PubMed]
14. Li, D.; Zhong, Z.; Ko, C.N.; Tian, T.; Yang, C. From mundane to classic: Sinomenine as a multi-therapeutic agent. *Br. J. Pharmacol.* **2025**, *182*, 2159–2180. [CrossRef] [PubMed]
15. Yang, X.; Xia, H.; Li, Y.; Cheng, Y.; Wang, Y.; Xia, Y.; Yue, Y.; Cheng, X.; Chu, Z. In vitro and ex vivo antioxidant activity and sustained release properties of sinomenine-loaded liposomes-in-hydrogel biomaterials simulating cells-in-extracellular matrix. *Nat. Prod. Commun.* **2022**, *17*. [CrossRef]
16. Zhu, M.; Wang, H.; Chen, J.; Zhu, H. Sinomenine improve diabetic nephropathy by inhibiting fibrosis and regulating the JAK2/STAT3/SOCS1 pathway in streptozotocin-induced diabetic rats. *Life Sci.* **2021**, *265*, 118855. [CrossRef] [PubMed]
17. Ding, C.; Li, Y.; Sun, Y.; Wu, Y.; Wang, F.; Liu, C.; Zhang, H.; Jiang, Y.; Zhang, D.; Song, X. Sinomenium acutum: A comprehensive review of its botany, phytochemistry, pharmacology and clinical application. *Am. J. Chin. Med.* **2022**, *50*, 1219–1253. [CrossRef] [PubMed]
18. Hou, W.; Huang, L.; Huang, H.; Liu, S.; Dai, W.; Tang, J.; Chen, X.; Lu, X.; Zheng, Q.; Zhou, Z. Bioactivities and mechanisms of action of sinomenine and its derivatives: A comprehensive review. *Molecules* **2024**, *29*, 540. [CrossRef] [PubMed]
19. Cheong, J.H.; Kim, C.Y.; Kim, J. Preparative isolation and purification of sinomenine from Sinomenium acutum by centrifugal partition chromatography. *J. Sep. Sci.* **2007**, *30*, 2105–2108. [CrossRef] [PubMed]
20. Jung, E.; Kim, J.; Kim, H.; Guo, S.; Lee, D.; Lim, G.; Syed, A.; Kim, W. Isolation of Alkaloids from Sinomenium acutum by Centrifugal Partition Chromatography and Their Ameliorating Effects on Dexamethasone-Induced Atrophy in C2C12 Myotubes. *Separations* **2023**, *10*, 470. [CrossRef]
21. Nigussie, G.; Zaib, S.; Dekebo, A.; Meressa, A.; Negassa, T.; Chanyalew, M.; Zarubaev, V.V.; Abebe, A.; Abebe, M.; Hunsen, M.; et al. Exploring the therapeutic potential of Kirkia tenuifolia Engl. stem bark extract and its bioactive compounds through experimental and computational approaches. *Sci. Rep.* **2025**, *15*, 38406. [CrossRef] [PubMed]
22. Fu, D.; Huang, J.; Li, K.; Chen, Y.; He, Y.; Sun, Y.; Guo, Y.; Du, L.; Qu, Q.; Miao, Y.; et al. Dihydrotestosterone-induced hair regrowth inhibition by activating androgen receptor in C57BL6 mice simulates androgenetic alopecia. *Biomed. Pharmacother.* **2021**, *137*, 111247. [CrossRef] [PubMed]
23. Owecka, B.; Tomaszewska, A.; Dobrzeniecki, K.; Owecki, M. The Hormonal Background of Hair Loss in Non-Scarring Alopecias. *Biomedicines* **2024**, *12*, 513. [CrossRef] [PubMed]
24. Seo, H.-S.; Lee, D.-J.; Chung, J.-H.; Lee, C.-H.; Kim, H.R.; Kim, J.E.; Kim, B.J.; Jung, M.H.; Ha, K.-T.; Jeong, H.-S. Hominis Placenta facilitates hair re-growth by upregulating cellular proliferation and expression of fibroblast growth factor-7. *BMC Complement. Altern. Med.* **2016**, *16*, 187. [CrossRef] [PubMed]
25. González Fernández, D.; Duchi, S.; Fernández Gómez, L.; León Sala, T.; Hajuj, A.; Molho, D.; Saada, N.A.; Molina Martínez, D.; Pérez-Fernández, A.; Goldstein, D. The Clinical Evaluation of Serum WS Biotin, a Novel Encapsulated Form of D-Biotin with Improved Water Solubility, for Anti-Hair Shedding Applications. A Prospective Single-Arm, Nonrandomized, Pretest−Posttest Study. *Health Sci. Rep.* **2025**, *8*, e70862. [CrossRef] [PubMed]
26. Begum, A.; Sandhya, S.; Kumar, A.N.; Ali, S.S. Evaluation of Herbal Hair Lotion Loaded with Rosemary for Possible Hair Growth in C57BL/6 mice. *Adv. Biomed. Res.* **2023**, *12*, 60. [CrossRef] [PubMed]
27. da Cruz, G.K.; Martins, M.I.M.; Antunes, F.T.T.; de Souza, A.H.; Wiilland, E.d.F.; Picada, J.N.; Brum, L.F.d.S. Evaluation of the efficacy and toxicity of oral and topical pumpkin oil on the hair growth of mice. *Acta Histochem.* **2022**, *124*, 151894. [CrossRef]
28. Baek, J.Y.; Kim, B.H.; Kim, D.-W.; Lee, W.-Y.; Kim, C.E.; Kim, H.-Y.; Pyo, J.; Park, E.-S.; Kang, K.S. Hair Growth Effect of DN106212 in C57BL/6 Mouse and Its Network Pharmacological Mechanism of Action. *Curr. Issues Mol. Biol.* **2023**, *45*, 5071–5083. [CrossRef] [PubMed]
29. Truong, V.-L.; Bak, M.J.; Lee, C.; Jun, M.; Jeong, W.-S. Hair regenerative mechanisms of red ginseng oil and its major components in the testosterone-induced delay of anagen entry in C57BL/6 mice. *Molecules* **2017**, *22*, 1505. [CrossRef] [PubMed]
30. Truong, V.-L.; Keum, Y.-S.; Jeong, W.-S. Red ginseng oil promotes hair growth and protects skin against UVC radiation. *J. Ginseng Res.* **2021**, *45*, 498–509. [CrossRef] [PubMed]

31. Müller-Röver, S.; Foitzik, K.; Paus, R.; Handjiski, B.; van der Veen, C.; Eichmüller, S.; McKay, I.A.; Stenn, K.S. A Comprehensive Guide for the Accurate Classification of Murine Hair Follicles in Distinct Hair Cycle Stages. *J. Investig. Dermatol.* **2001**, *117*, 3–15. [CrossRef] [PubMed]
32. Cai, Y.; Jia, Z.; Zhang, Y.; Kang, B.; Chen, C.; Liu, W.; Li, W.; Zhang, W. Cell-free fat extract restores hair loss: A novel therapeutic strategy for androgenetic alopecia. *Stem Cell Res. Ther.* **2023**, *14*, 219. [CrossRef] [PubMed]
33. Kim, Y.N.; Lee, J.S.; Park, M.G.; Kim, Y.J.; Lee, S.M.; Hwang, K.H.; Yang, M.H.; Kwon, B.-O.; Rho, J.-R.; Jeong, E.J. Phytochemical Profiling of the Halophyte Artemisia fukudo Makino and Its In Vitro Effects on Androgen-Related Pathways Associated with Benign Prostatic Hyperplasia and Alopecia. *ChemistryOpen* **2026**, *15*, e202500481. [CrossRef] [PubMed]
34. Zhou, D.; Liu, Z.; Jie, X.; Zhu, X. Advances in Research on Concentrated Growth Factor Applications for Androgenetic Alopecia Treatment: A Review. *Med. Sci. Monit. Int. Med. J. Exp. Clin. Res.* **2025**, *31*, e948054. [CrossRef] [PubMed]
35. Botchkarev, V.; Handjiski, B.; Metz, M.; Hibino, T.; Soma, T.; Dotto, G.; Paus, R. Control of murine hair follicle regression (catagen) by TGF-betal in vivo. *FASEB J.* **2000**, *14*, 752–760. [CrossRef] [PubMed]
36. Xiang, S.; Wu, X.; Xiang, Y. Sinomenine suppressed keratinocyte proliferation and imiquimod-induced psoriasis-like dermatitis by regulating lncRNA XIST. *Skin. Pharmacol. Physiol.* **2022**, *35*, 328–342. [CrossRef] [PubMed]
37. Guan, T.; Li, N.; Xu, X.; Xiong, D.; Wang, B.; Xiao, L.; Yang, W.; Chu, G.; Yusuf, A.; Zhang, J.; et al. Involvement of the Keap1-Nrf2-ARE pathway in the antioxidant activity of sinomenine. *Arch. Biochem. Biophys.* **2024**, *753*, 109928. [CrossRef] [PubMed]
38. Anouar, E.; Calliste, C.A.; Košinová, P.; Di Meo, F.; Duroux, J.L.; Champavier, Y.; Marakchi, K.; Trouillas, P. Free Radical Scavenging Properties of Guaiacol Oligomers: A Combined Experimental and Quantum Study of the Guaiacyl-Moiety Role. *J. Phys. Chem. A* **2009**, *113*, 13881–13891. [CrossRef] [PubMed]
39. Zhang, B.; Chen, T. Local and systemic mechanisms that control the hair follicle stem cell niche. *Nat. Rev. Mol. Cell Biol.* **2024**, *25*, 87–100. [CrossRef]
40. Natarelli, N.; Gahoonia, N.; Sivamani, R.K. Integrative and Mechanistic Approach to the Hair Growth Cycle and Hair Loss. *J. Clin. Med.* **2023**, *12*, 893. [CrossRef] [PubMed]
41. Jang, S.K.; Joo, S.S. Promotional effects of Sargassum fusiforme fractions on hair growth via in vitro and in vivo models. *J. Biomed. Transl. Res.* **2014**, *15*, 72–77. [CrossRef]
42. Wang, J.; Wang, L.; Gao, S.; Li, X. Recent Advances in the Role of Fibroblast Growth Factors in Hair Follicle Growth. *Biomolecules* **2025**, *15*, 1198. [CrossRef] [PubMed]
43. Cuevas-Diaz Duran, R.; Martinez-Ledesma, E.; Garcia-Garcia, M.; Bajo Gauzin, D.; Sarro-Ramírez, A.; Gonzalez-Carrillo, C.; Rodríguez-Sardin, D.; Fuentes, A.; Cardenas-Lopez, A. The Biology and Genomics of Human Hair Follicles: A Focus on Androgenetic Alopecia. *Int. J. Mol. Sci.* **2024**, *25*, 2542. [CrossRef] [PubMed]
44. Liang, A.; Fang, Y.; Ye, L.; Meng, J.; Wang, X.; Chen, J.; Xu, X. Signaling pathways in hair aging. *Front. Cell Dev. Biol.* **2023**, *11*, 1278278. [CrossRef] [PubMed]
45. Papukashvili, D.; Liu, C.; Rcheulishvili, N.; Xie, F.; Wang, X.; Feng, S.; Sun, X.; Zhang, C.; Li, Y.; He, Y.; et al. DKK1-targeting cholesterol-modified siRNA implication in hair growth regulation. *Biochem. Biophys. Res. Commun.* **2023**, *668*, 55–61. [CrossRef] [PubMed]
46. Kovanecz, I.; Gelfand, R.; Sharifzad, S.; Ohanian, A.; DeCastro, W.B.; Cooper, C.; Lin, G.; Lue, T.; Gonzalez-Cadavid, N.F. Evaluation of the In Vitro Damage Caused by Lipid Factors on Stem Cells from a Female Rat Model of Type 2 Diabetes/Obesity and Stress Urinary Incontinence. *Int. J. Mol. Sci.* **2020**, *21*, 5045. [CrossRef] [PubMed]
47. Ma, Y.-Q.; Sun, Z.; Li, Y.-M.; Xu, H. Oxidative stress and alopecia areata. *Front. Med.* **2023**, *10*, 1181572. [CrossRef] [PubMed]
48. Suchonwanit, P.; Kositkuljorn, C.; Pomsoong, C. Alopecia areata: An autoimmune disease of multiple players. *ImmunoTargets Ther.* **2021**, *2021*, 299–312. [CrossRef] [PubMed]
49. Jiang, S.; Li, S.; Pang, S.; Liu, M.; Sun, H.; Zhang, N.; Liu, J. A systematic review: Sinomenine. *Heliyon* **2024**, *10*, e29976. [CrossRef] [PubMed]
50. Pérez-Mora, S.; Ocampo-López, J.; Gómez-García, M.D.; Pérez-Ishiwara, D.G. BFNB Enhances Hair Growth in C57BL/6 Mice through the Induction of EGF and FGF7 Factors and the PI3K-AKT-β-Catenin Pathway. *Int. J. Mol. Sci.* **2023**, *24*, 12110. [CrossRef] [PubMed]
51. Van Neste, D. Placebo-controlled dose-effect studies with topical minoxidil 2% or 5% in male-patterned hair loss treated with oral finasteride employing an analytical and exhaustive study protocol. *Skin. Res. Technol.* **2020**, *26*, 542–557. [CrossRef] [PubMed]
52. Olsen, E.A.; Weiner, M.S. Topical minoxidil in male pattern baldness: Effects of discontinuation of treatment. *J. Am. Acad. Dermatol.* **1987**, *17*, 97–101. [CrossRef] [PubMed]

Disclaimer/Publisher's Note: The statements, opinions and data contained in all publications are solely those of the individual author(s) and contributor(s) and not of MDPI and/or the editor(s). MDPI and/or the editor(s) disclaim responsibility for any injury to people or property resulting from any ideas, methods, instructions or products referred to in the content.